

Density of states in SF bilayers with arbitrary strength of magnetic scattering

D. Yu. Guskova^{*1)}, A. A. Golubov⁺, M. Yu. Kupriyanov^{*}, A. Buzdin[△]

⁺Department of Applied Physics, University of Twente, 7500 AE Enschede, Netherlands

^{*}Nuclear Physics Institute, Moscow State University, 119992 Moscow, Russia

[△]Institut Universitaire de France and Condensed Matter Theory Group, CPMOH, University Bordeaux 1, UMR 5798, CNRS, F-33405 Talence Cedex, France

Submitted 13 March 2006

We developed the self-consistent method for the calculation of the density of states $N(\varepsilon)$ in the SF bilayers. It based on the quasi-classical Usadel equations and takes into account the suppression of superconductivity in the S layer due to the proximity effect with the F metal, as well as existing mechanisms of the spin dependent electron scattering. We demonstrate that the increase of the spin orbit or spin flip electron scattering rates results in completely different transformations of $N(\varepsilon)$ at the free F layer interface. The developed formalism has been applied for the interpretation of the available experimental data.

PACS: 74.45.+c, 74.50.+r

It is well known that superconductivity can be induced into a non-superconducting material from a superconductor due to proximity effect. In the superconductor (S) – normal metal (N) bilayers thus induced minigap and the shape of the density of states (DOS) at free N metal interface $N(\varepsilon)$ depends on the values of the suppression parameters of SN interface and relation between the N layer thickness and the decay length of the N metal [1–4]. The existence of the minigap has been confirmed experimentally in a variety of the proximity SN systems (see e.g. [5–8] and references therein). In the superconductor – ferromagnet (F) bilayers there are additional bulk F-layer parameters which influence on $N(\varepsilon)$. They are the exchange field H and the electron spin scattering processes. The exchange field tends to align all electron spins along the field axis. It splits the minigap and density of states for spin up and spin down electrons (see [9–11] for the reviews). The experimental study of the proximity effect in SF systems [12–16] and Josephson effect in SFS junctions [17, 18] reveals that besides the exchange field the additional pair-breaking magnetic mechanism, namely, spin dependent electron scattering, should be taken into account for the data interpretation.

There are three types of the spin dependent electron scattering in the ferromagnet – spin-orbit interaction and spin-flip processes which may happen along the exchange field direction and in the plane perpendicular to it. Previously the influence of the parallel spin-flip

and spin-orbit scattering mechanisms on $N(\varepsilon)$ had been considered in some limiting cases (rigid boundary conditions at SF interface, limits of large or small F layer thickness) [19, 20].

In this paper we for the first time developed the self-consistent method for the calculation of the density of states in SF bilayers. It is based on the quasi-classical Usadel equations and takes into account the suppression of the superconductivity in the S layer due to the proximity effect with the F metal, as well as all three mechanisms of the spin dependent electron scattering. We have demonstrated that the developed formalism can be applied for understanding the $N(\varepsilon)$ data obtained in superconductors with the antiferromagnet ordering. We consider the SF bilayer consisting of two dirty metals. They are a superconductor of the thickness d_s and a thin ferromagnet d_f adjoined at $x=0$. All physical quantities depend on coordinate x perpendicular to the SF boundary. The exchange field is parallel to the SF interface plane. DOS can be calculated from the Usadel equations. To proceed further it is convenient to use the θ parametrization $G(\omega, x) = \cos \theta(\omega, x)$, $F(\omega, x) = \sin \theta(\omega, x)$, where G and F are normal and anomalous Green functions. The magnetic and spin-orbit scattering mix up the up and down spin states which couples the Usadel equations for the Green functions with the opposite spin directions. In the F layer ($x < 0$) it gives the system of the two equations

$$-\frac{D_f}{2} \frac{\partial^2 \theta_{f1(2)}}{\partial x^2} + \left(\omega \pm iH + \frac{1}{\tau_z} \cos \theta_{f1(2)} \right) \sin \theta_{f1(2)} + \frac{1}{\tau_x} \sin(\theta_{f1} + \theta_{f2}) \pm \frac{1}{\tau_{so}} \sin(\theta_{f1} - \theta_{f2}) = 0, \quad (1)$$

¹⁾e-mail: dariamessage@yandex.ru

and in the S layer ($x > 0$) the Usadel equations stay uncoupled

$$-\frac{D_s}{2} \frac{\partial^2 \theta_{s1(2)}}{\partial x^2} + \omega \sin \theta_{s1(2)} = \Delta(x) \cos \theta_{s1(2)}, \quad (2)$$

where θ_1 and θ_2 correspond to the Green functions with the opposite spin directions, $\omega = \pi T(2n+1)$ are the Matsubara frequencies, D_s (D_f) is the diffusion coefficient in S (F) layer, H is the exchange field energy in F layer, $\Delta(x)$ is the superconducting energy gap which is zero in F layer. Here we use the self-consistent method to resolve the Usadel equations which takes into account the decrease of the energy gap Δ in the S layer from its bulk value along x -axis towards the boundary due to the proximity effect. The scattering times are labelled here as τ_z , τ_x and τ_{so} , where $\tau_{z(x)}$ corresponds to the magnetic scattering parallel (perpendicular) to the quantization axis and τ_{so} corresponds to the spin-orbit scattering.

In the S layer the Usadel equations are completed with the self-consistency equation

$$\Delta(x) \ln t + t \sum_{\omega=0}^{\omega=\infty} \left[\frac{2\Delta(x)}{\omega} - \sin \theta_{s1} - \sin \theta_{s2} \right] = 0, \quad (3)$$

where $t = T/T_c$, T_c is the bulk superconducting temperature. Here and further we work with the normalized energy parameters $\Delta \equiv \Delta/\pi T_c$, $\omega \equiv \omega/\pi T_c$, $H \equiv H/\pi T_c$, and for the length parameters in F layer $x \equiv x/\xi_n$, $\xi_n = \sqrt{D_f/2\pi T_c}$, and in S layer $x \equiv x/\xi_s$, $\xi_s = \sqrt{D_s/2\pi T_c}$. The scattering parameter notations are $\alpha_z = (\tau_z \pi T_c)^{-1}$, $\alpha_x = (\tau_x \pi T_c)^{-1}$, $\alpha_{so} = (\tau_{so} \pi T_c)^{-1}$.

The boundary conditions at FS interface have the form

$$\gamma_B \frac{\partial \theta_{f1(2)}}{\partial x} \Big|_{x=-0} = \sin(\theta_{s1(2)} - \theta_{f1(2)}),$$

$$\frac{\gamma_B}{\gamma} \frac{\partial \theta_{s1(2)}}{\partial x} \Big|_{x=+0} = \sin(\theta_{s1(2)} - \theta_{f1(2)}), \quad (4)$$

and at free edges

$$\frac{\partial \theta_{f1(2)}}{\partial x} \Big|_{x=-d_f} = 0, \quad \frac{\partial \theta_{s1(2)}}{\partial x} \Big|_{x=d_s} = 0, \quad (5)$$

where $\gamma = \sigma_n \xi_s / \sigma_s \xi_n$, $\sigma_{n(s)}$ is the conductivity of the F(S) layer, $\gamma_B = R_b \sigma_n / \xi_n$, R_b is the specific resistance of the SF interface.

For the arbitrary layers thicknesses, interface parameters, γ , γ_B , and magnetic scattering parameters the equations (1)-(5) have been solved numerically using the self-consistent two step iterative procedure (for ref. see [1-3]). In the first step we calculate the order parameter coordinate dependence $\Delta(x)$, in the Matsubara technique using the self-consistent condition in the S layer.

Due to the proximity effect $\Delta(x)$ decreases towards the SF interface. Then by proceeding to the analytical extension in (1), (2) over the energy parameter $\omega \rightarrow -i\varepsilon$ and using $\Delta(x)$ dependence obtained in the previous step we find the Green functions by repeating the iterations until the convergency is reached. The density of states $N(\varepsilon) = N_{\uparrow}(\varepsilon) + N_{\downarrow}(\varepsilon)$ can be found as

$$N_{\uparrow(\downarrow)}(\varepsilon) = 0.5N(0)Re \cos \theta_{1(2)}, \quad (6)$$

where $N_{\uparrow(\downarrow)}$ is the DOS for the one spin direction and N is the total DOS.

The numerically obtained energy dependencies of DOS in F layer at the free F boundary are presented on Figs.1-7. At $H = 0$ (Fig.1) we reproduce the well

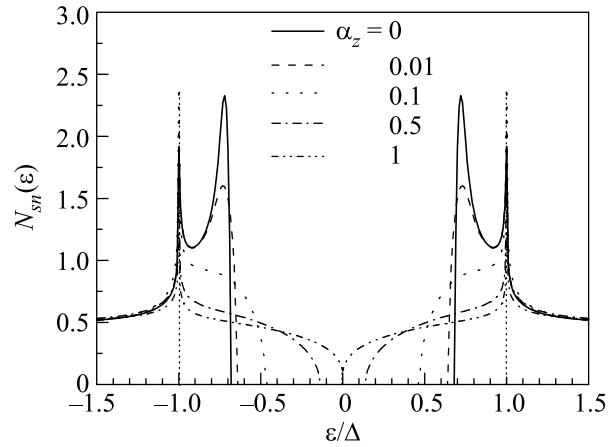


Fig.1. The case of the parallel magnetic scattering in the S/N bilayer ($H/\pi T_c = 0$). Spin up energy DOS variation in the N layer for several values of the magnetic scattering parameter α_z and for the fixed $\gamma_B = 5$, $\gamma = 0.05$, $d_f/\xi_n = 0.2$, $d_s/\xi_s = 10$, $\alpha_x = 0$, $\alpha_{so} = 0$

known mini gap existing in SN bilayer [1-3]. The presence of the uniaxial magnetic scattering tends to smooth the BCS peaks in the DOS. Figure 2 demonstrates the DOS evolution for the spin up electrons for different parameters α_z where the full black curve corresponds to the usual splitted peaks within the energy gap due to the exchange field in the absence of any magnetic scattering. By adding the magnetic scattering aligned with the exchange field direction one can see the smearing of the sharp peaks with the gradual closing of the induced energy gap in the F layer. It is interesting to note that the symmetry of the spin resolved DOS in respect of Fermi energy ($\varepsilon = 0$) does not exist in the presence of magnetic scattering.

Figure 3 demonstrates the influence of the perpendicular magnetic scattering on the energy DOS variation within the energy gap. Total DOS for both spin direc-

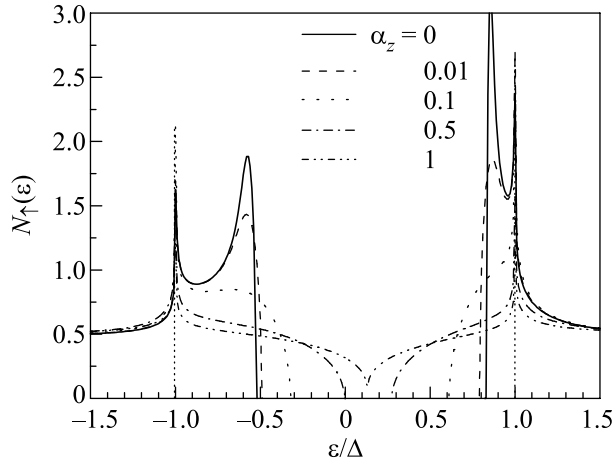


Fig.2. The case of parallel magnetic scattering. Spin up Energy DOS variation in the F layer for several values of the magnetic scattering parameter α_z and for the fixed $H/\pi T_c = 0.2$, $\gamma_B = 5$, $\gamma = 0.05$, $d_f/\xi_n = 0.2$, $d_s/\xi_s = 10$, $\alpha_x = 0$, $\alpha_{so} = 0$

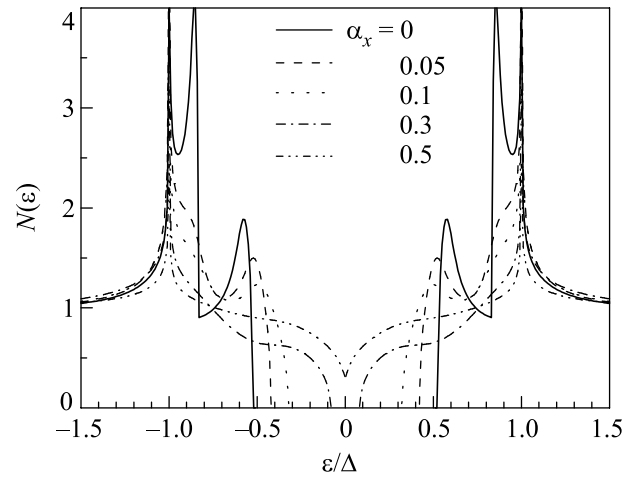


Fig.4. The case of the perpendicular magnetic scattering. Total DOS energy variation in the F layer for several values of the magnetic scattering parameter α_x and for the fixed $H/\pi T_c = 0.2$, $\gamma_B = 5$, $\gamma = 0.05$, $d_f/\xi_n = 0.2$, $d_s/\xi_s = 10$, $\alpha_z = 0$, $\alpha_{so} = 0$

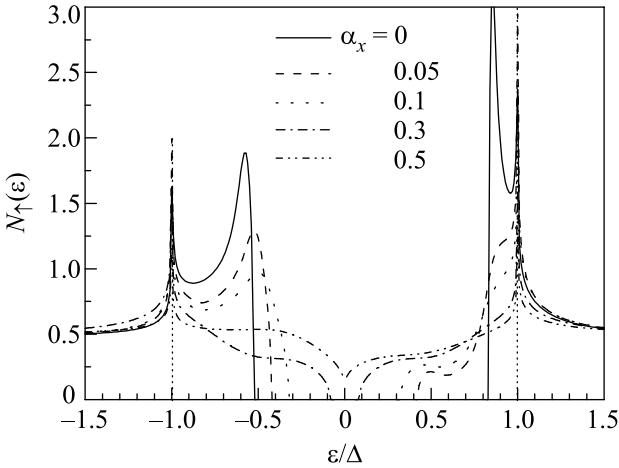


Fig.3. The case of the perpendicular magnetic scattering. Spin up energy DOS variation in the F layer for several values of the magnetic scattering parameter α_x and for the fixed $H/\pi T_c = 0.2$, $\gamma_B = 5$, $\gamma = 0.05$, $d_f/\xi_n = 0.2$, $d_s/\xi_s = 10$, $\alpha_z = 0$, $\alpha_{so} = 0$

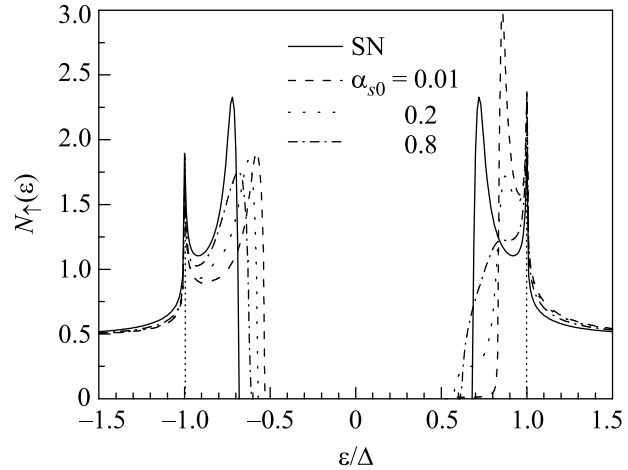


Fig.5. The case of spin-orbit scattering. Spin up energy DOS variation in the F layer for several values of the magnetic scattering parameter α_{so} and for the fixed $H/\pi T_c = 0.2$, $\gamma_B = 5$, $\gamma = 0.05$, $d_f/\xi_n = 0.2$, $d_s/\xi_s = 10$, $\alpha_z = 0$, $\alpha_x = 0$. Black curve corresponds to the SN case

tions for the different values of the perpendicular magnetic scattering parameter α_x is plotted in Fig.4. The peaks in DOS are slowly moving towards the zero energy that can be explained as the presence of some additional splitting field besides the ordinary exchange field in ferromagnet. As in the case of parallel magnetic scattering the peaks are smoothed out and the energy gap disappears. For the small magnetic scattering times τ_z and τ_x the DOS tends to its bulk value in the ferromagnet.

Figures 5 and 6 depict the spin up and total DOS for different parameters of spin-orbit scattering, correspondingly. It can be seen that in contrast to the mag-

netic scattering described above the spin-orbit scattering tends to decrease the effect of the peak splitting within the energy gap caused by the ferromagnetic exchange field. Black curves in Fig.5 and 6 correspond to the zero exchange field (SN structure case). The smaller the spin-orbit scattering time the closer the curve to the superconductor/normal metal case and two minigap behavior degenerate to the one minigap curve as in the SN structure.

It is interesting to mention the peculiarity in DOS dependence in the presence of the spin-orbit scattering. As

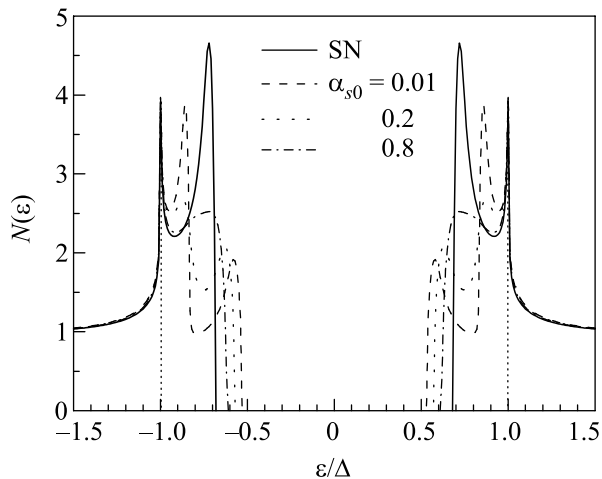


Fig.6. The case of spin-orbit scattering. Total DOS energy variation in the F layer for several values of the magnetic scattering parameter α_{so} and for the fixed $H/\pi T_c = 0.2$, $\gamma_B = 5$, $\gamma = 0.05$, $d_f/\xi_n = 0.2$, $d_s/\xi_s = 10$, $\alpha_z = 0$, $\alpha_x = 0$. Black curve corresponds to the SN case

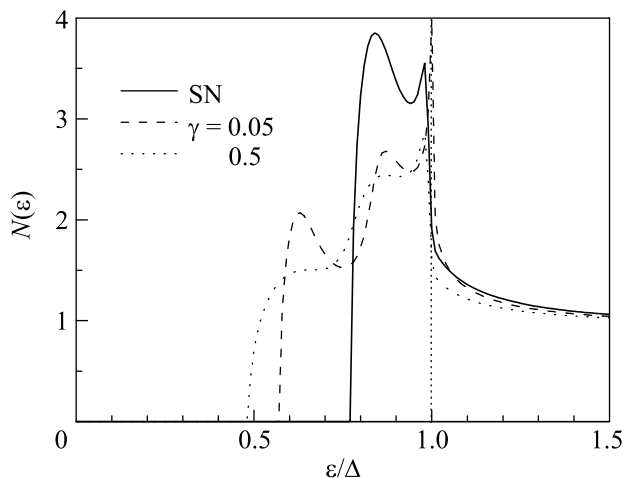


Fig.7. The case of spin-orbit scattering. Total DOS energy variation in the F layer for $\tau_{so}^{-1} = H$ and for the fixed $H/\pi T_c = 0.2$, $\gamma_B = 5$, $d_f/\xi_n = 0.2$, $d_s/\xi_s = 10$, $\alpha_z = 0$, $\alpha_x = 0$. Black curve corresponds to the SN case with $\gamma = 0.5$. Dashed and dotted curves correspond to two different values of the γ parameter

it was shown in [21, 22] in the presence of the spin-orbit scattering for the parameter $\tau_{so}^{-1} = H$ the solution of the Usadel equation changes its characteristic behavior from the oscillating one to the damping decay, that should also cause the changes in the energy DOS variation. Figure 7 demonstrates the appearance of the plateau instead of peak in DOS for $\tau_{so}^{-1} = H$ for some parameter γ when it is large enough to diminish the penetration of superconductivity into the F layer. For the particular set of parameters (H , γ_B , d_s , d_f) used for calculation of the

graph in Fig.7 this transformation occurs approximately at $\gamma \approx 0.5$.

Recently, the coexistence of the magnetic and superconducting order in nickel borocarbides was studied in several laboratories experimentally. Such compounds as $\text{ErNi}_2\text{B}_2\text{C}$ and $\text{TmNi}_2\text{B}_2\text{C}$ both being the superconducting materials demonstrate radically different magnetic properties. Local tunnelling microscopy at low temperatures revealed considerable difference in the local superconducting density of states behavior. In contrast with $\text{TmNi}_2\text{B}_2\text{C}$ [23] compound where DOS has its usual BCS type, $\text{ErNi}_2\text{B}_2\text{C}$ [24] measurements show the non zero conductance and thereby the non zero DOS within the energy gap.

To find the possible explanation of such a difference we propose the following model. We believe that in $\text{ErNi}_2\text{B}_2\text{C}$ compound the magnetic order near the surface is absent even when the antiferromagnetic phase appears in the bulk. This may be related with some atomic compositional disorder near the surface and modified exchange interaction between magnetic moments near the surface. Consequently, to describe the surface properties of superconducting $\text{ErNi}_2\text{B}_2\text{C}$, the model of a thin film with the relatively strong magnetic scattering on the top of the bulk superconductor without magnetic scattering seems to be quite reasonable.

Using the developed algorithm for the SF bilayer, we may assume the exchange field $H = 0$ as in the paramagnetic case and $\gamma = 1$, $\gamma_B = 0$ for the actual absence of the boundary. Fig.8a demonstrates the calculated DOS behavior at $x = -d_f$ in the presence of the magnetic scattering which destroys the usual BCS behavior. For $\text{ErNi}_2\text{B}_2\text{C}$ having easy plane magnetic anisotropy we take $1/\tau_z = 0$ and $1/\tau_x = 1/\tau_y = 1/\tau$. Fig.8b corresponds to the case without magnetic scattering. It can be seen that both black theoretical curves are in a good agreement with the experimental data of [24] (Fig.1a and Fig.2b). The difference between $\text{ErNi}_2\text{B}_2\text{C}$ and $\text{TmNi}_2\text{B}_2\text{C}$ curves may be related with the important difference in their Neel temperatures (6 K and 1.5 K, respectively). The lower T_N may lead to the much smaller magnetic scattering in $\text{TmNi}_2\text{B}_2\text{C}$.

In conclusion we demonstrate that the increase of spin orbit or spin flip electron scattering rates results in completely different transformations of $N(\varepsilon)$ at free F layer interface. The increase of τ_z^{-1} results in the continuous suppression of the peaks in the density of states accompanied by the closing of the energy gap. The increase of τ_x^{-1} additionally leads to the shift of the peaks towards the zero energy which looks like the action of some additional exchange field in the ferromagnet. Contrary to that the increase of τ_{so}^{-1} does not result in the

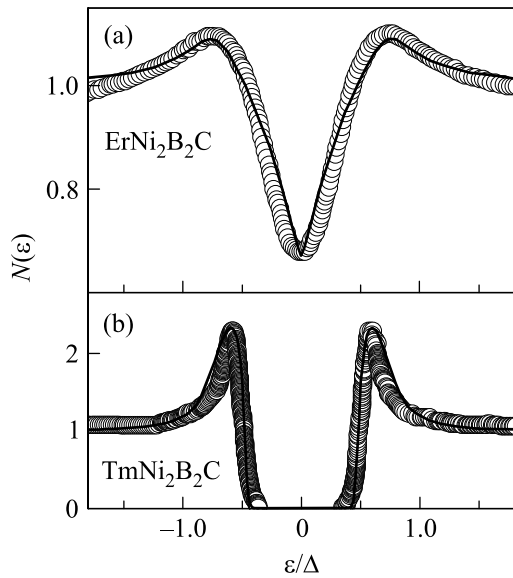


Fig.8. Theoretical fit of the experimental data of [24] (Fig.1). Plot parameters: $H = 0$, $\gamma = 1$, $\gamma_B = 0$, $d_s \gg \xi_s$, $\alpha_z = \alpha_{so} = 0$. a) $T = 0.15$ K, $T_c = 11$ K, $d_f = 0.35\xi_n$ and magnetic scattering parameter $\alpha_x = 0.95$; b) $T = 0.8$ K, $T_c = 10.5$ K, $d_f = 0.6\xi_n$, no magnetic scattering

closing of the energy gap and tends to decrease the Zeeman peaks splitting.

All calculations have been done in a self-consistent way in the frame of the Usadel equations. The developed formalism has been successfully applied for the interpretation of the data obtained in the superconductors with the antiferromagnet ordering.

This work has been supported by RFBR project # 06-02-90865 We acknowledge the support by French EGIDE programme # 10197RC, ESF PI-Shift Programme and NanoNed programme under project TCS # 7029. We are grateful to H. Suderow for useful discussions and providing experimental data prior to publication.

1. A. A. Golubov and M. Yu. Kupriyanov, J. Low. Temp. Phys. **70**, 83 (1988).
2. A. A. Golubov and M. Yu. Kupriyanov, ZhETF **96**, 1420 (1989) [Sov. Phys. JETP **69**, 805 (1989)].

3. A. A. Golubov, E. P. Houwman, J. G. Gijsbertsen et al., Phys. Rev. B **51**, 1073 (1995).
4. W. Belzig, C. Bruder, and G. Schon, Phys. Rev. B **54**, 9443 (1996).
5. S. Gueron, H. Pothier, Norman O. Birge et al., Phys. Rev. Lett. **77**, 3025 (1996).
6. N. Moussy, H. Courtois, and B. Pannetier, Europhys. Lett. **55**, 861 (2001).
7. E. Scheer, W. Belzig, Y. Naveh et al., Phys. Rev. Lett. **86**, 284 (2001).
8. L. Cretinon, A. Gupta, B. Pannetier, and H. Courtois, Physica C **404**, 103 (2004).
9. A. Buzdin, Rev. Mod. Phys. **77**, 935 (2005).
10. A. A. Golubov, M. Yu. Kupriyanov, and E. Il'ichev, Rev. Mod. Phys. **76**, 411 (2004).
11. F.S. Bergeret, A.F. Volkov, and K.B. Efetov, Rev. Mod. Phys. **77**, 1321 (2005).
12. T. Kontos, M. Aprili, J. Lesueur, and X. Gison, Phys. Rev. Lett. **86**, 304 (2001).
13. L. Cretinon, A. K. Gupta, H. Sellier et al., Phys. Rev. B **72**, 024511 (2005).
14. S. Reymond, P. SanGiorgio, M. R. Beasley et al., Phys. Rev. B **73**, 054505 (2006).
15. A. Cottet and W. Belzig, Phys. Rev. B **72**, 180503(R) (2005).
16. C. Cirillo, L. S. Prischepa, M. Salvato, and C. Attanasio, Phys. Rev. B **72**, 144511 (2005).
17. V. A. Oboznov, V. V. Bol'ginov, A. K. Feofanov et al., arXiv: cond-mat/0508573.
18. M. Faure, A. I. Buzdin, A. A. Golubov, and M. Yu. Kupriyanov, Phys. Rev. B **73**, 064505 (2006).
19. M. J. DeWeert and G. B. Arnold, Phys. Rev. B **30**, 5048 (1984).
20. M. J. DeWeert, Phys. Rev. B **38**, 732 (1988).
21. E. A. Demler, G. B. Arnold, and M. R. Beasley, Phys. Rev. B **55**, 15174 (1997).
22. S. Kuplevakhskii and I. Fal'ko, Theor. Mat. Fiz. **86**, 188 (1990).
23. H. Suderow, P. Martinez-Samper, N. Luchier et al., Phys. Rev. B **64**, 020503(R) (2001).
24. M. Crespo, H. Suderow, S. Vieira et al., Phys. Rev. Lett. **96**, 027003 (2006).